Acta Oceanol. Sin., 2014, Vol. 33, No. 7, P. 56–64
DOI: 10.1007/s13131-014-0504-8
http://www.hyxb.org.cn
E-mail: hyxbe@263.net

A numerical study on seasonal variations of the thermocline in the South China Sea based on the ROMS

FAN Wei[1]*, SONG Jinbao[1], LI Shuang[2]

[1] Key Laboratory of Ocean Circulation and Waves, Institute of Oceanology, Chinese Academy of Sciences, Qingdao 266071, China
[2] Department of Ocean Science and Engineering, Zhejiang University, Hangzhou 310058, China

Received 26 March 2012; accepted 26 November 2013

Abstract

On the basis of the regional ocean modeling system (ROMS), the seasonal variations of the thermocline in the South China Sea (SCS) were numerically investigated. The simulated hydrodynamics are in accordance with previous studies: the circulation pattern in the SCS is cyclonic in winter and anticyclonic in summer, and such a change is mostly driven by the monsoon winds. The errors between the modeled temperature profiles and the observations obtained by cruises are quite small in the upper layers of the ocean, indicating that the ocean status is reasonably simulated. On the basis of the shapes of the vertical temperature profiles, five thermocline types (shallow thermocline, deep thermocline, hybrid thermocline, double thermocline, and multiple thermocline) are defined herein. In winter, when the northeasterly monsoon prevails, most shallow shelf seas in the northwest of the SCS are well mixed, and there is no obvious thermocline. The deep region generally has a deep thermocline, and the hybrid or double thermocline often occurs in the areas near the cold eddy in the south of the SCS. In summer, when the southwesterly monsoon prevails, the shelf sea area with a shallow thermocline greatly expands. The distribution of different thermocline types shows a relationship with ocean bathymetry: from shallow to deep waters, the thermocline types generally change from shallow or hybrid to deep thermocline, and the double or multiple thermocline usually occurs in the steep regions. The seasonal variations of the three major thermocline characteristics (the upper bound depth, thickness, and intensity) are also discussed. Since the SCS is also an area where tropical cyclones frequently occur, the response of thermocline to a typhoon process in a short time scale is also analyzed.

Key words: thermocline, South China Sea, ROMS, typhoon

Citation: Fan Wei, Song Jinbao, Li Shuang. 2014. A numerical study on seasonal variations of the thermocline in the South China Sea based on the ROMS. Acta Oceanologica Sinica, 33(7): 56–64, doi: 10.1007/s13131-014-0504-8

1 Introduction

The South China Sea (SCS), which is located in the tropical-subtropical brim of the western north Pacific Ocean, is the largest semi- enclosed marginal sea in this area. It extends from the equator to 22°N and from 99° to 121°E, which has a total area of 3.5×10^6 km^2. Geographically, the SCS connects to the western Philippine Sea (WPS) through the Luzon Strait (>2 000 m) in the east and connects to the Sulu and Java Seas through the Mindoro Strait (approximately 200 m) and Karimata Straits (<50 m) in the south. It also connects to the East China Sea (ECS) through the Taiwan Strait (<100 m) in the north. A deep north–east/south-west oriented abyssal basin is located in the central-east part of the SCS with a maximum depth of 5 420 m. Because of the location and topography, the SCS has the features of both shelf seas and tropical oceans. The bathymetry of the SCS is shown in Fig. 1.

Along with the advancement of studies on the climate change, researchers have started to pay more attention to the upper layers of the ocean. The thermocline, which is the transitional layer between the mixed layer and the deep water layer, is essential to the dynamics of the upper ocean. Beyond that, the thermocline also has a significant influence on the underwater acoustic communication (by influencing the sound channel), fishery and oceanic engineering (the thermocline is a place where the internal waves are prone to take place, and this may cause great damages to the oceanic facility). Therefore, the thermocline (especially the seasonal thermocline) is becoming a central issue that researchers focus on.

The pioneer work on the thermocline in the SCS can be traced to Mao and Qiu (1964), whose study indicates that the thermocline characteristics of the SCS are similar to those of the deep oceans. Most relevant previous works on the SCS thermocline mainly refer to some particular regions, such as the shelf seas in the north part of the SCS (e.g., Mao and Qiu, 1964; Liu, 1989) and the Nansha Islands together with its adjacent waters (e.g., Qiu and Cai, 2000; Li et al., 2000).

Guan (1981) analyzed the relationship between the thermocline and hydrodynamics of the SCS, indicating that basic circulations are determined by the orientation of the SCS thermocline. Liu et al. (2000) investigated the seasonal variations

Foundation item: The National Basic Research Program of China under contract Nos 2011CB403501 and 2012CB417402; the Fund for Creative Research Groups by National Natural Science Foundation of China under contract No. 41121064; the Knowledge Innovation Programs of the Chinese Academy of Sciences under contract No. KZCX2-YW-Q07-02.
*Corresponding author, E-mail: fanjieyu@163.com

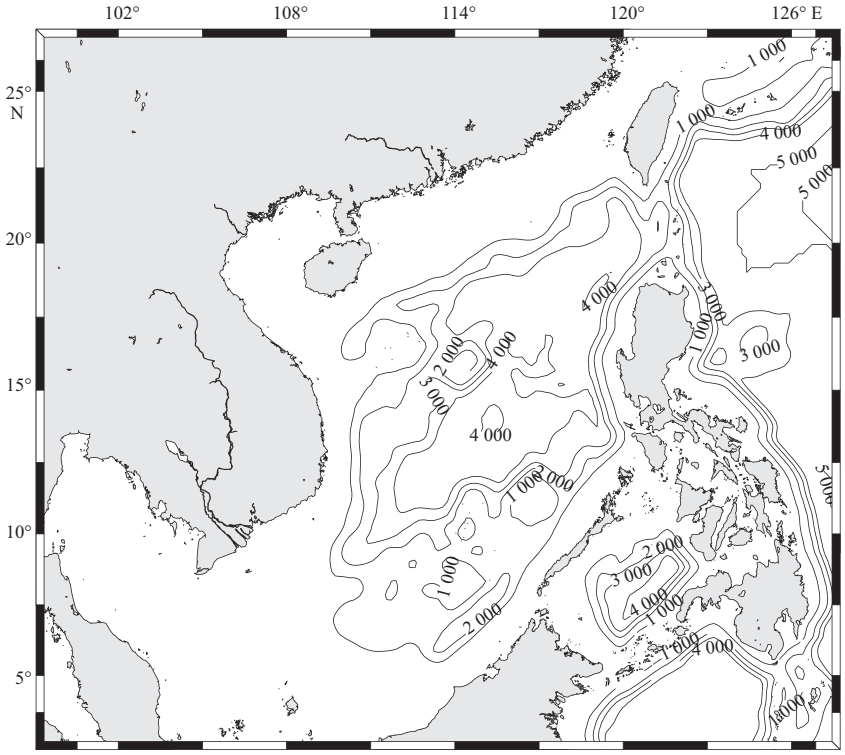

Fig.1. The model domain and bathymetry (m) of the SCS (2°–27°N, 99°–128°E).

of thermocline in the deep sea region of the SCS by using historical data (1907 to 1990). The thermocline in the SCS is the thinnest and weakest in winter, the thickest in spring, and the strongest in summer and fall. Owing to the upper Ekman transport caused by monsoon over the SCS, the thermocline slopes upward (downward) in winter (summer) from northwest to southeast. The intrusion of the Kuroshio and mesoscale eddies can remarkably affect the depth, thickness and intensity of the thermocline. Liu et al. (2001) analyzed the seasonal and intra-seasonal variability of the thermocline in the central part of the SCS using the time series data of temperature from three buoys (February, 1998–March, 1999). The seasonal variation of the thermocline in the central SCS is mainly caused by the seasonal variation of the surface wind stress and the net heat flux. While the intra-seasonal variation of the thermocline is mainly caused by the mesoscale eddies and the intra-seasonal variation of the net heat flux.

Zhou et al. (2004) studied the distribution and characteristics of the SCS thermocline based on the accumulated historical cruises data. Using 0.05°C/m as the lowest criterion of the thermocline intensity, the shallow thermocline distributes in the northwest shelf seas with notable seasonal variations. The deep thermocline exists in the abyssal basin all year round, but this has little relationship with the atmospheric conditions. Zhang et al. (2006) studied the distribution of thermocline in the China seas based on the historical investigating data from the year 1900 to 2004 at the SCS and the sea area around Taiwan, China. There are four stages of the shallow thermocline variations in the north of the SCS: increasing (March–May), strong (June–August), decreasing (September–October) and no thermocline (November–February). The upper bound of thermocline and thickness are parallel to the coastal line, showing an ascending trend from north to south and west to east. Lan et al. (2006) analyzed the spatial distributions and seasonal variabilities of the thermocline depth in the SCS based on the GDEM (generalized digital environmental model) temperature and salinity data. It is shown from the analysis results that the circulation and multi-eddy structure in the SCS have significant effects on the thermocline in the SCS.

The research works reviewed above are essential for our understanding of the thermocline and its characteristics in the SCS. However, most previous studies are usually confined to some specific sea areas, and studies on the thermocline of the whole SCS are relatively rare. Taking a comprehensive view on the seasonal variations of the thermocline in the SCS (i.e., distribution of different types of thermocline, the upper bound depth, thermocline thickness and intensity) may help us further understand its environment and hydrodynamics. In this study, we simulated the status of the SCS by utilizing the regional ocean modeling system (ROMS). After validating the model results, an analysis of the thermocline based on the model output in the SCS was given. Since the SCS is also an area where tropical cyclones frequently form or pass, the response of the thermocline to a typhoon process is also discussed.

The paper is organized as follows: First, the model and its validation are described in Section 2, while some definitions referring to the thermocline and how to calculate the thermocline are given in Section 3; the results and discussions are shown in Section 4; and Section 5 presents the conclusions.

2 Model and validation

2.1 *Model configuration*

The ROMS (Rutgers version 3.2, http://www.myroms.org) (Haidvogel et al., 2008) utilized in this study is a three-dimensional primitive equation ocean circulation model derived from the serial *s*-coordinate Rutgers University model (SCRUM). The model has a free surface and utilizes a vertically stretched terrain-following coordinate (*s*-coordinate). The ROMS model is one of the most popular models used in today's ocean modeling, which has been widely used in many fields (e.g., ocean dynamics, marine ecosystems, sediments and air-sea interaction).

The model domain (Fig. 1) in this study (2°–27° N, 99°–128° E) covers most of the SCS, the southern part of the ECS, and part of the western Pacific brim. The horizontal resolution is 10′×10′, and there are 50 *s*-levels in the vertical (with enhanced resolution in the upper ocean). The bathymetry was derived from the Etopo2 (version 2), while the air-sea flux and wind stress data were from NCEP/DOE Reanalysis 2. The GODAE daily GHRSST data were used to constrain the model. The open boundary conditions were provided by the ECCO (estimating the circulation & climate of the ocean) products. Four main tidal constituents (M_2, S_2, K_1 and O_1) were imposed on the three open boundaries. The turbulence closure scheme was the Mellor and Yamada Level 2.5. The simulation was initialized in January 2000, and the initial field is also derived from the corresponding ECCO data. The model was spun up for 8 a from initialization to December 2007, and the outputs of the year 2008 and 2009 served as materials for model validation and future analysis. The reason why the year 2008 and 2009 are selected as the simulation period is that the observations to validate the model are obtained by two cruises carried out during the two years.

2.2 *Model validation*

2.2.1 *Circulation*

The seasonal circulation pattern in the SCS and its adjacent seas has been investigated by many researchers (e.g., Dale, 1956; Pohlmann, 1987; Li et al., 1992; Shaw and Chao, 1994; Takano et al., 1998). A review of these studies was made by Hu et al. (2000), and the upper layer circulation pattern summarized from previous studies is shown in Figs 2a and b. Notice that some hydrodynamic features (e.g., the existence of the anticyclonic eddy

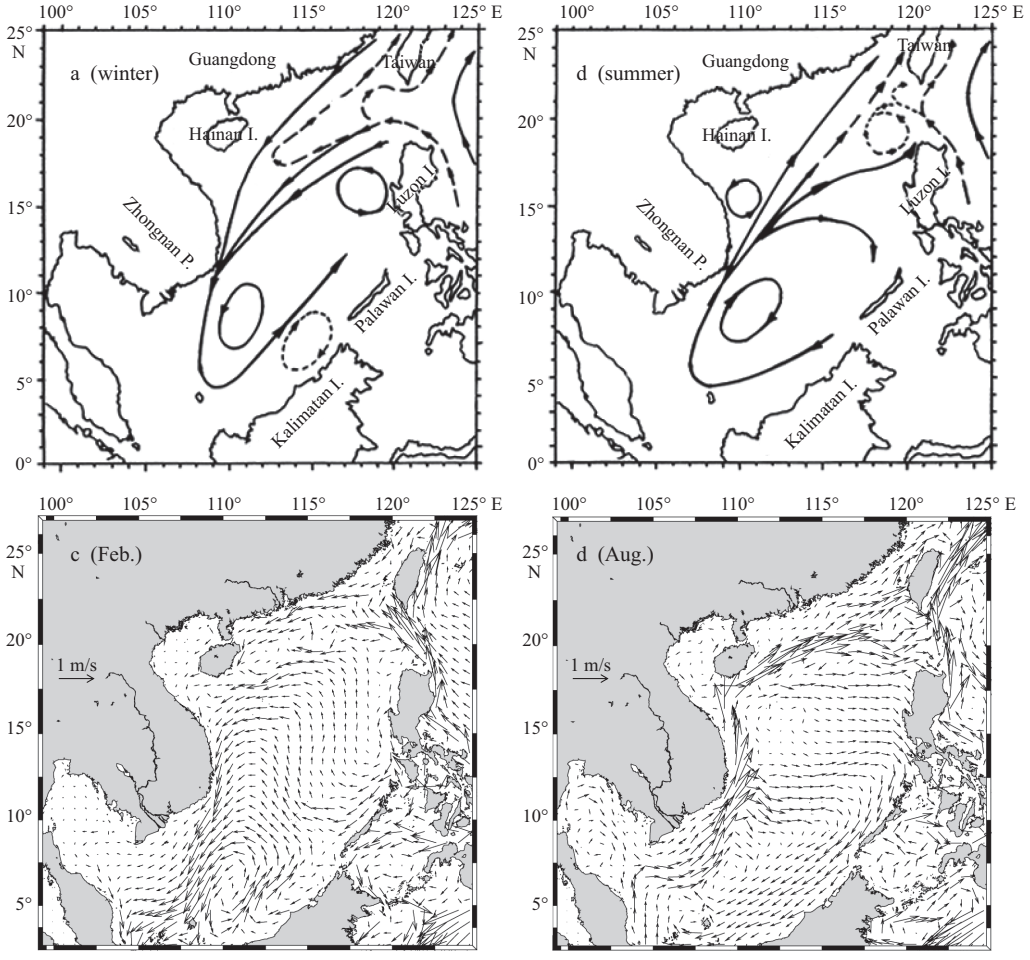

Fig.2. Comparison of the circulation pattern in the upper ocean between previous studies and the simulation. The circulation patterns in the upper ocean summarized from previous studies by Hu et al. (2000) are shown in a (winter) and b (summer); the modeled surface currents (10 m, monthly mean) are shown in c (February) and d (August).

and the cyclonic eddy shown in short dash line in Figs 2a and b, respectively) still need further confirmation. The seasonal SCS circulation is mostly affected by the monsoon winds, while the northern part of the SCS circulation is also related to water exchanges between the SCS and the ECS through the Taiwan Strait and between the SCS and the Kuroshio through the Luzon Strait.

A comparison of the circulation pattern between Hu et al.'s (2000) summary and the simulation results of the year 2008 (monthly mean) is shown in Fig. 2. It should be noted that the former is based on climatology while our simulation is carried out for a specific period of time, so there can be some differences in between. Nevertheless, the main circulation patterns and hydrodynamic characteristics can be captured by the model. As for the upper layer circulation, it is cyclonic in winter but anticyclonic in summer, and this is in accordance with previous studies. In winter, there is a cyclonic eddy to the southeast of the Zhongnan Peninsula, and the South China Sea Warm Current (SCSWC) in the south off the Guangdong coast can also be distinguished from the model results. In summer, the circulation pattern is opposite to that in winter because of the opposite direction of the monsoon, and an anticyclonic eddy appears to the southeast of the Zhongnan Peninsula.

However, in winter, the Luzon cold eddy cannot be captured clearly in Fig. 2c. To check its existence, the circulation in a depth of 50 m around Luzon Island is shown in Fig. 3. The Luzon cyclone shows a double eddy structure and can be clearly distinguished from Fig. 3a (white ellipses). The double eddy structure has been reported by a few studies (i.e., Yang and Liu, 1998; Sun and Liu, 2011), and it consists of two cyclonic eddies: one is located to the west of Luzon Island, and the other is to the northwest of Luzon Island. Owing to upwelling, the water temperature within the Luzon cold eddy is a few degrees lower than the surroundings. Beyond that, there is also a small cyclone eddy near the Lingayen Gulf (Fig. 3a). Because the water temperature within this eddy is close to that of the adjacent areas, it may be a temporal eddy. As we know, the Luzon cold eddy usually lasts from October to May and is the strongest in January. Thus, in summer, there is no obvious cold water area near Luzon Island (Fig. 3b).

2.2.2 *Temperature profiles*

Since the thermocline is a feature derived from the temperature profile, the validation of the temperature fields in the upper ocean is crucial. Two cruises were carried out during September 2008 and June 2009, respectively, and the temperature profiles of 91 sites in total are observed by the CTD. The site distributions in the two cruises are shown in Fig. 4, and the errors between simulation and observations are shown in Table 1. Since the thermocline usually exists in the upper layers of the ocean,

Table 1. Errors between the simulation and observations

Cruise 200809												
Depth/m	10	20	30	40	50	60	80	100	150	200	250	300
MAE/°C	0.69	0.55	0.52	0.68	0.79	0.93	0.84	0.81	1.13	1.26	1.04	0.87
Standard deviation of absolute error/°C	0.50	0.37	0.38	0.45	0.63	0.76	0.78	0.60	0.88	0.68	0.54	0.62
Cruise 200906												
Depth/m	10	20	30	40	50	60	80	100	150	200	250	300
MAE/°C	1.11	0.99	0.82	0.77	0.84	1.00	1.39	1.59	1.52	1.14	0.81	0.69
Standard deviation of absolute error/°C	0.71	0.85	0.78	0.76	0.63	0.71	0.97	1.09	1.08	0.84	0.61	0.61

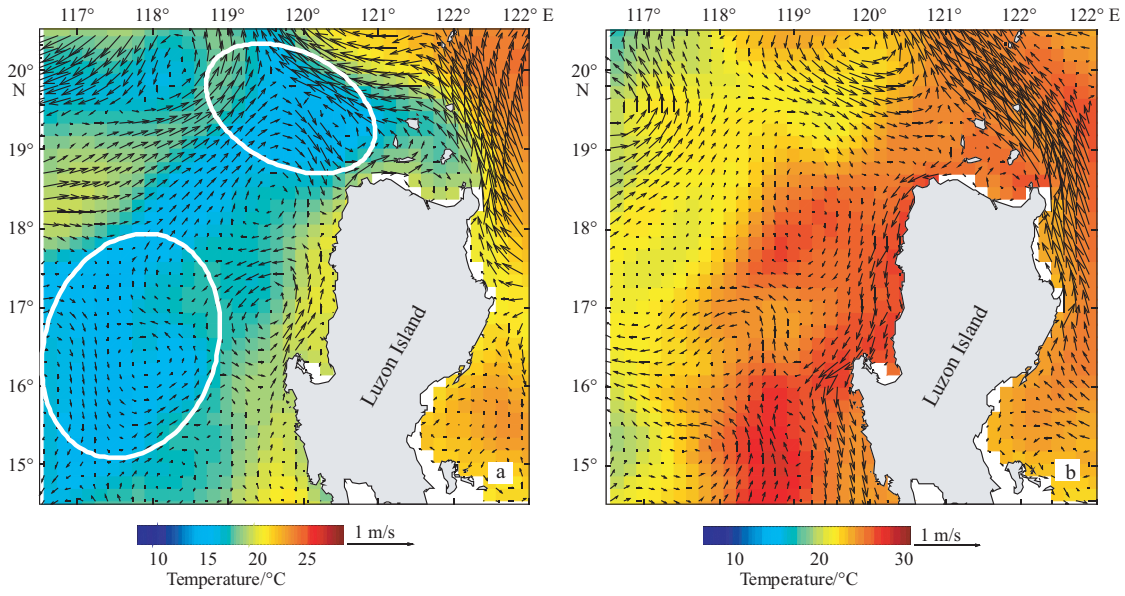

Fig.3. The monthly mean temperature (color) and current velocity (vector) in a depth of 50 m around Luzon Island. a. February and b. August.

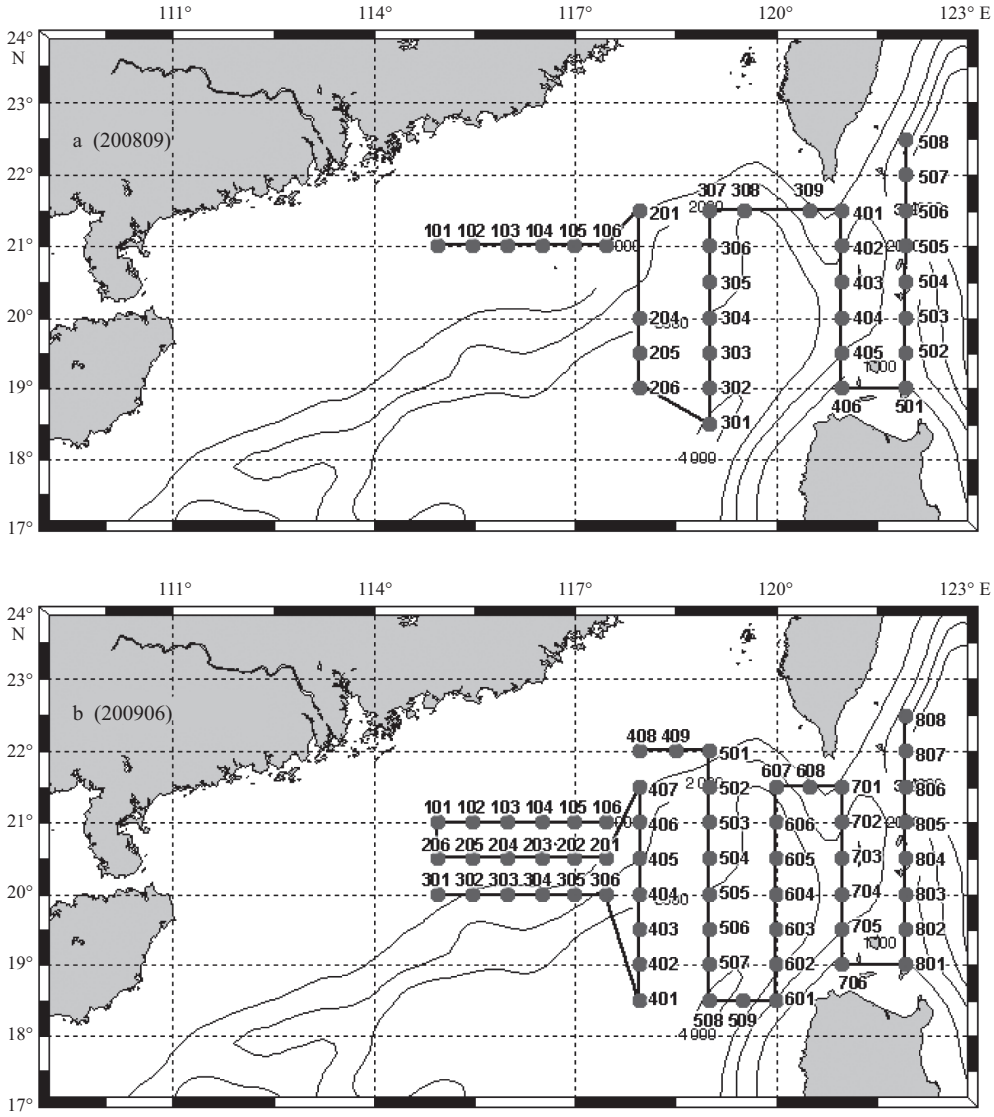

Fig.4. Distribution of sites in cruises 200809 and 200906, respectively. a. 33 sites and b. 58 sites.

the comparison only refers to the upper 300 m. Basically, both the mean absolute error (MAE) and the standard deviation of the absolute error in most layers are less than 1°C, which means the temperature fields are reasonably simulated.

3 Definitions of different thermocline types

The thermocline types can be classified according to their formation mechanism, variation period, the air-sea interaction theory, etc. In this study, the classification of thermocline is based on the shapes of the vertical temperature profiles. Since the SCS has the features of both shelf seas and tropical oceans, and since major areas are deeper than 200 m, for the sake of continuity, a unified vertical temperature gradient of 0.05 °C/m was taken as the lowest criterion of the thermocline judgment. Hereby, several thermocline types are defined as follows, which is similar to Zhou et al. (2004).

(1) For the shallow thermocline the upper bound is shallower than 50 m, and the thickness is thinner than 50 m;

(2) For the deep thermocline the upper bound is deeper than 50 m;

(3) For the hybrid thermocline the upper bound is shallower than 50 m while the thickness is thicker than 50 m;

(4) For the double thermocline there are two separate thermoclines;

(5) For the multiple thermocline there are more than two thermoclines.

To distinguish between the shallow thermocline, which has a great seasonal variation, and the basically stable deep thermocline, the upper bound 50 m was chosen as the criterion based on the characteristics of seasonal thermocline in shelf seas off China. The hybrid thermocline indicates that both the lower bound of the shallow thermocline and the upper bound of the deep thermocline are not obvious and their thicknesses are approximate. In this situation, the thermocline thickness is usually large while the thermocline intensity is relatively weak.

The phenomenon of temperature inversion has been reported by a few studies in the SCS in recent years. However, this phenomenon usually occurs in the northeast coastal area from October to May and only occupies a small proportion of the SCS (Hao et al., 2010). Therefore, the temperature inversion is ignored in this study. Since the thermocline might be discontinuous in a small vertical length, the programming for calculating the thermocline is quite complicated. Main processes are as follows. First, the vertical temperature gradients are calculated layer by layer. If the layers meet the criterion continuously, then they are merged into one layer. Otherwise, if the interval between the two layers is smaller than a specific length (10 m, if the upper bound is shallower than 50 m; 30 m, if the upper bound is deeper than 50 m), a judgment will be given after precombining the two layers. After that, if the vertical temperature gradient meets the criterion, then the two layers are merged into one layer; if not, the two layers will be judged to determine whether one of them is only a perturbation of the profile. Generally, for the deep thermocline, the thickness should be greater than 20 m; and for the shallow thermocline, the thickness should be greater than 10 m.

4 Results and discussions

Since the regular patterns of the thermocline in the SCS do not significantly vary between different years, the following analysis referring to the seasonal variations of the thermocline types and characteristics is based on the simulation result of the year 2008.

4.1 *Thermocline types*

The distributions of different thermocline types are shown in Fig. 5, and they are quite different between winter and summer. In winter, the seawater in the shallow shelf sea areas are well mixed in vertical, thus in most of these areas there have no thermoclines, and in most deep regions in the central and in northeast of the SCS there have deep thermoclines. There are hybrid and double thermoclines near the cold eddy to the southeast of the Zhongnan Peninsula, which indicates that the upwelling caused by the positive vorticity raises the upper bound of the thermocline.

In summer, the sea area which has a shallow thermocline in the shelf region greatly expands. The deep thermocline in most areas is replaced by the hybrid thermocline. It is shown that there is a relationship between the distribution of different thermocline types and the bathymetry: from shallow to deep waters, the thermocline types generally change from shallow or hybrid to deep thermoclines, and the double or multiple thermocline usually occurs in the steep regions.

4.2 *Major characteristics of the thermocline*

The upper bound depth, thickness, and intensity are three major characteristics of the thermocline. The seasonal variations of the upper bound depth is shown in Figs 6a (February) and b (August). In winter, the northeasterly monsoon prevails, and the upper bound of the thermocline is deeper in continental slope and the coastal area where the current is strong (e.g., the location of L1, 17°30′N, 114°E). Since the total circulation pattern in winter is cyclonic, the upper bound is much shallower in the interior area of the SCS and the areas near the cold eddy. When the prevailing wind direction is opposite in summer, similar to the circulation pattern, the upper bound depth of the thermocline also shows an opposite distribution. That is, it is much deeper in the interior area than in the surroundings, and this is basically caused by the anticyclonic circulations. Generally, the upper bound of the thermocline in major areas is shallower than 50 m in summer. L2 (10°N, 114°E) is a typical location which lies in the basin interior. In February, the circulation pattern is cyclonic and the upper bound depth at L2 is 35 m. In summer (August), the circulation pattern is reversed and the upper bound becomes much deeper (59 m).

The seasonal variations of the thermocline thickness are shown in Figs 6c (February) and d (August). Because the mixed layer is thicker in winter than in summer, the thermocline is relatively compressed during this period, which results in a thinner thermocline. Spatially, the interior area of the SCS is much thicker than that in the coastal areas, suggesting that permanent thermoclines exist in the deep region. The seasonal variations of the thermocline intensity are shown in Figs 6e (February) and f (August). For the shallow shelf seas, the seasonal variations of the thermocline intensity are remarkable. The thermocline intensity is weak (even no thermocline) in winter, but strong in summer (the maximal value is higher than 0.3°C/m). And for

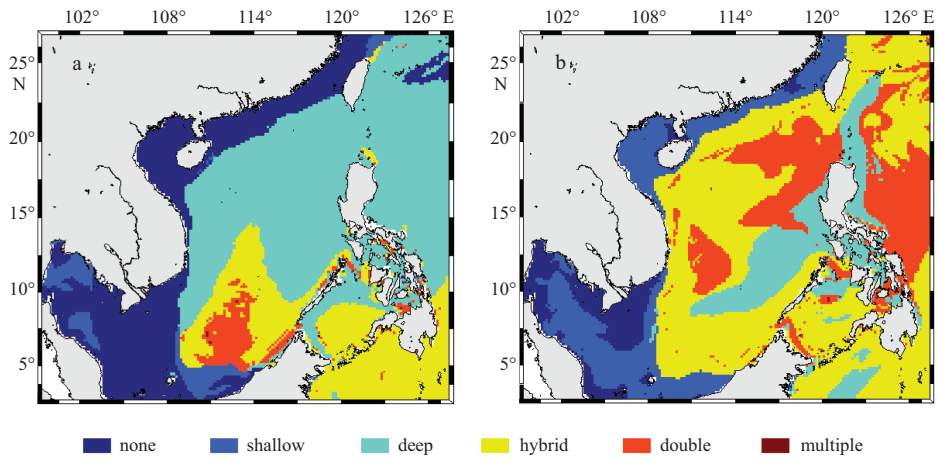

Fig.5. The distributions of different thermocline types in winter (a) and summer (b).

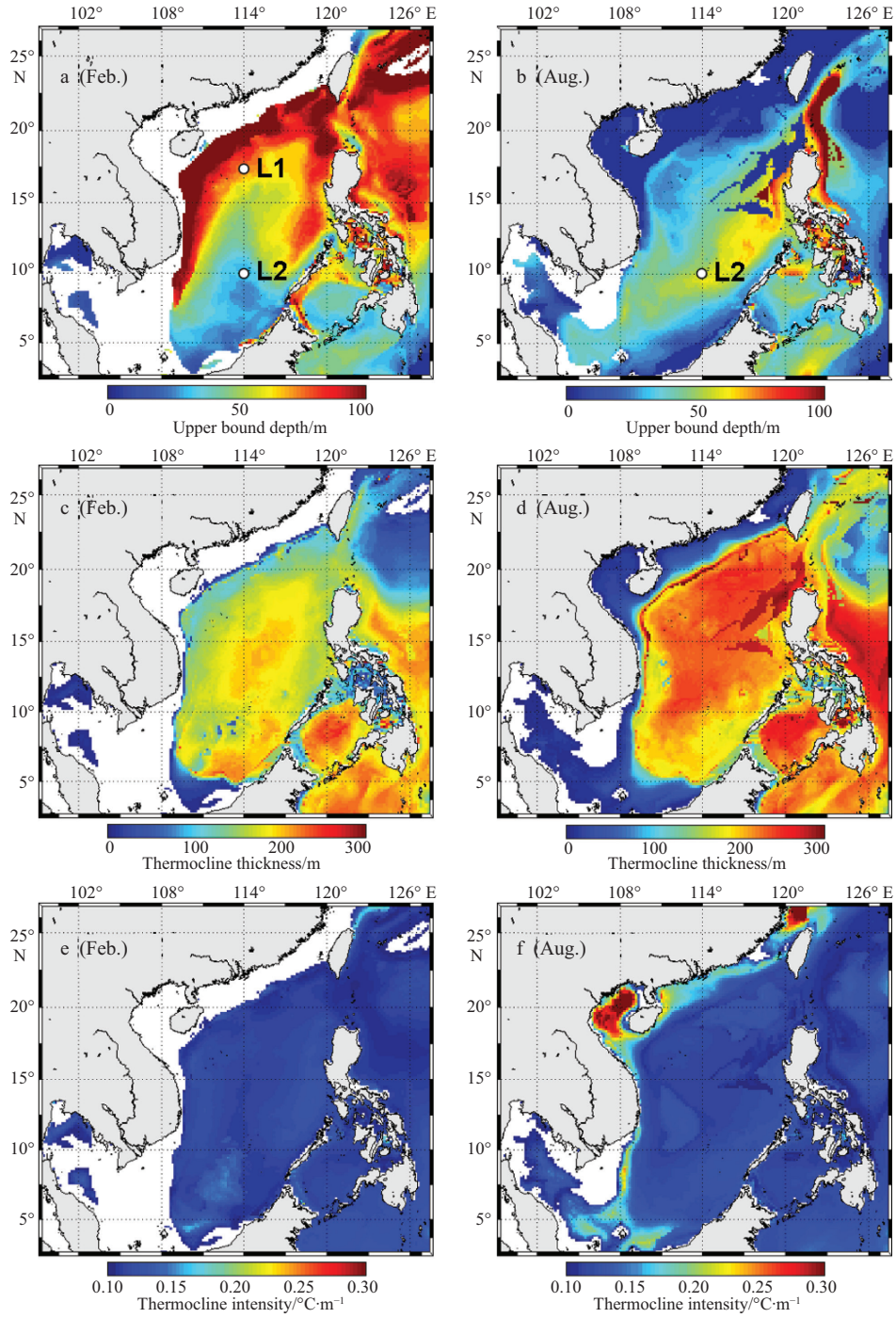

Fig.6. Seasonal variations of the three thermocline characteristics. The seasonal variations of the upper bound depth are shown in a (February) and b (August); the seasonal variations of the thermocline thickness are shown in c (February) and d (August); the seasonal variations of the thermocline intensity are shown in e (February) and f (August).

the deep interior area, the thermocline intensity is relatively stable because of the existence of the permanent thermocline.

4.3 *The response of thermocline to a typhoon process in a short time scale*

The SCS is an area where tropical cyclones or typhoons frequently form and pass. During the past several decades, on average, eight typhoons have passed the northern SCS each year (from UNISYS Weather homepage; http://weather.unisys.com/hurricane). A typhoon is a storm system with strong positive wind stress curl, and obviously this strong air-sea interaction has a significant impact on the ocean dynamics and the heat fluxes. The positive wind stress curl can induce upwelling via the Ekman pumping. Zhou et al. (1995) analyzed the seasonal

variations of surface and subsurface layer temperatures in the SCS. It is shown that Ekman pumping induced by wind stress curl can influence the vertical movement of the thermocline, and the response time of thermocline to the wind stress curl in the SCS is about 20–30 d, which is much faster than that of the tropical Pacific, 2–3 months (Wang et al., 2000). How does the thermocline respond to a typhoon process? How long is the response time? During the periods of the two cruises, several typhoons happened to pass the SCS. Taking these typhoons as an example, this paper investigates the response of thermocline to typhoons based on the model results, which are shown in Fig. 6. The selected two sites (K304 of cruise 200809 and K502 of cruise 200906) are in or very close to the typhoon track, and the mean absolute error between the observations and modeled values of the two sites are 0.72 and 0.58 °C, respectively.

From September 22, 2008 to September 24, 2008, the typhoon "Hagupit" passed the SCS from the Luzon Strait to the Guangdong coast. On Site K304 (20°N, 119°E, in cruise 200809), the wind speed was small before September 6, and the surface water was heated remarkably (Fig. 7a). During this period of time, the upper bound of the thermocline could even reach the surface. From September 7 to 20, the wind speed increased, and the surface layer was well mixed. The upper bound depth showed a trend opposite the wind speed. The upper bound and its adjacent isotherm (29 °C) became shallower, while the deeper isotherms (26 °C and 24 °C) in the thermocline were still stable. This shows that a big wind process can only influence the top layers. When "Hagupit" passed by, both the wind speed and the wind stress curl increased. The deeper isotherms (26 °C and 24 °C) were raised clearly by the upwelling caused by the wind stress curl, which indicates that a typhoon process cannot only induce strong mixing in the top layers, but also influences the waters that are much deeper than the upper bound of the thermocline. Obviously, this influence decreases with depth. In addition, the denser isotherms in the thermocline strengthen the local thermocline intensity. According to the isotherms shown in Fig. 7a, the upper bound of the thermocline and its adjacent isotherms respond to typhoon with virtually no delay, while the deeper waters in the thermocline respond to typhoon with a delay of approximately 1–2 d.

Figure 7b shows another similar case in June 2009. The difference is that two typhoons ("Linfa" and "Nangka") passed Site

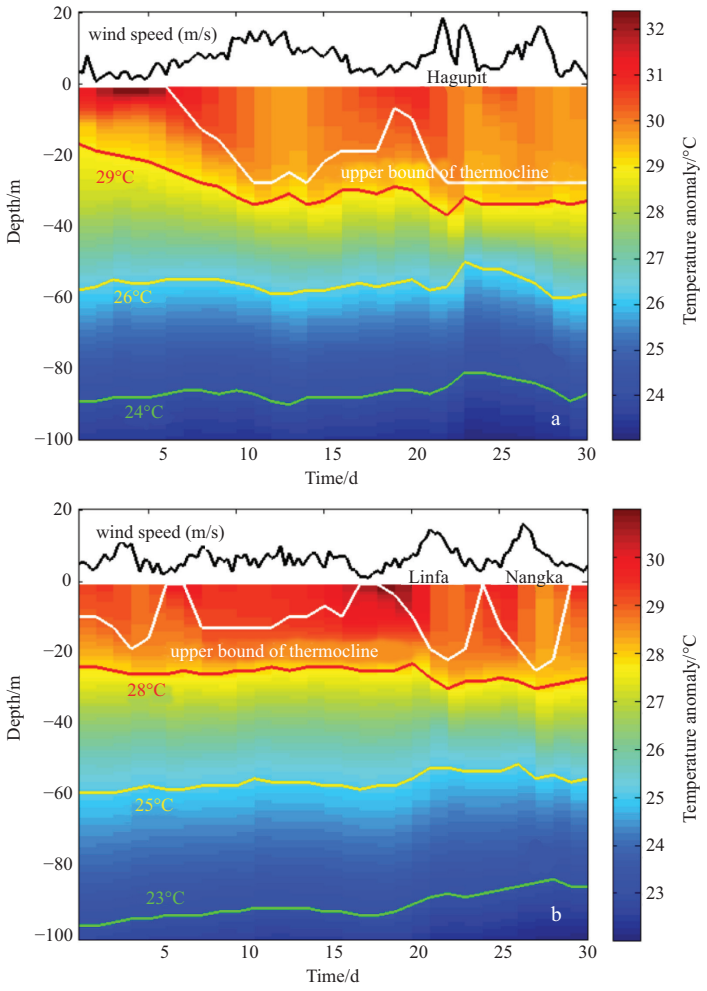

Fig.7. The response of thermocline to typhoons. a. 20.0°N, 119.0°E and b. 21.5°N, 118.0°E. The black and white lines indicate the wind speed and the upper bound depth, respectively. Hagupit, Linfa and Nangka are the names of three typhoons.

K502 (21°30′N, 118°E, in cruise 200906) continuously, and the thermocline responses followed in a continuous way.

5 Conclusions

The seasonal variations of the thermocline in the SCS are investigated based on an oceanic model. According to the shapes of the vertical temperature profiles, five thermocline types are defined. Hereby, the seasonal variations of the thermocline distributions were investigated. In winter, most shallow shelf seas in the northwest of the SCS are well mixed, and the deep region generally has a deep thermocline. In summer, the shelf sea area with a shallow thermocline greatly expands, and there is a relationship between the thermocline distributions and the bathymetry: from shallow to deep waters, the thermocline types generally change from shallow or hybrid to deep thermoclines.

The three major thermocline characteristics were also discussed in this study, and they are summarized as follows.

(1) For the upper bound depth, in winter the upper bound is deeper in continental slopes and in the coastal areas where the current is strong, while it is much shallower in the interior area. In summer, the upper bound depth shows an opposite distribution.

(2) For the thermocline thickness, the thermocline is thinner in winter than in summer, and it is thicker in the interior area of the SCS than in the coastal areas.

(3) For the thermocline intensity, the thermocline intensity is weak (even no thermocline) in the shallow shelf seas in winter, but strong in summer; the thermocline intensity is relatively stable in the deep interior area.

This paper also discusses the response of thermocline to a typhoon process in a short time scale. A typhoon process cannot only deepen the upper bound depth but also influences deeper waters. During a typhoon process, the isotherms in the thermocline are compressed, which results in intensified vertical temperature gradients. The upper bound of the thermocline and its adjacent isotherms responds to typhoon quickly, while the deeper waters in the thermocline respond to typhoon with a delay of approximately 1–2 d.

Acknowledgements

The authors would like to thank the High Performance Computing Center in the Institute of Oceanology, Chinese Academy of Sciences for supplying the computing environment.

References

Dale W L. 1956. Wind and drift current in the South China Sea. The Malayan Journal of Tropical Geography, 8: 1–31

Guan Bingxian. 1999. Phenomenon of the inversion thermocline in winter in the coastal water of the west of East China Sea and its relation to circulation. Journal of Oceanography of Huanghai & Bohai Seas (in Chinese), 17(2): 1–7

Haidvogel D B, Arango H, Budgell W P, et al. 2008. Ocean forecasting in terrain-following coordinates: formulation and skill assessment of the regional ocean modeling system. Journal of Computational Physics, 227: 3595–3624

Hao Jiajia, Chen Yongli, Wang Fan. 2010. Temperature inversion in China seas. J Geophys Res, 115: C12025, doi: 10.1029/2010JC006297

Hu Jianyu, Kawamura H, Hong Huasheng, et al. 2000. A review on the currents in the South China Sea: seasonal circulation, South China Sea Warm Current and Kuroshio intrusion. Journal of Oceanography, 56: 607–624

Lan Jian, Bao Ying, Yu Fei, et al. 2006. Seasonal variabilities of the circulation and thermocline depth in the South China Sea deep water basin. Advance in Marine Science (in Chinese), 24(4): 436-445

Li Peiliang, Qi Jianhua, Fang Xinhua. 2000. The characteristics of the sea water transition layer in the investigated area of Nansha Islands in Nov. 1997. Tansactions of Oceanology and Limnology (in Chinese), 1: 1–7

Li Rongfeng, Zeng Qingcun, Ji Zhongzhen, et al. 1992. Numerical simulation for a northeastward flowing current from area off the eastern Hainan Island to Tsugaru/Soya Strait. La Mer, 30: 229–238

Liu Guifang. 1989. Distribution characteristics of temperature, salinity and density in the continental shelf off east Guangdong during July 1987. Tropic Oceanology (in Chinese), 8(2): 39–47

Liu Qinyu, Jia Yinglai, Liu Penghui, et al. 2001. Seasonal and intraseasonal thermocline variability in the central South China Sea. Geophys Res Lett, 28(23): 4467–4470

Liu Qinyu, Yang Haijun, Wang Qi. 2000. Dynamic characteristics of seasonal thermocline in the deep sea region of the South China Sea. Chinese J Oceanol, 118(2): 104–109

Mao Hanli, Qiu Daoli. 1964. National Oceanic Comprehensive Survey Report: Thermocline, Halocline, Pycnocline Phenomena in China Coastal waters Waters (in Chinese). Beijing: China Science Press, 116

Pohlmann T. 1987. A three dimensional circulation model of the South China Sea. In: Nihoul J C J , Jamart B M, eds. Three-Dimensional Models of Marine and Estuarine Dynamics. New York: Elsevier, 245–268

Qiu Zhang, Cai Shuqun. 2000. Distribution characteristics of mean sea temperature relative to thermocline in deep water of Nansha Islands sea area. Tropic Oceanology (in Chinese), 19(4): 10–13

Shaw P T, Chao S Y. 1994. Surface circulation in the South China Sea. Deep-Sea Res Pt I, 40(11/12): 1663–1683

Sun Chengxue, Liu Qinyu. 2011. Double eddy structure of the winter Luzon cold eddy based on satellite altimeter data. Journal of Tropical Oceanography (in Chinese), 30(3): 9–15

Takano K, Harashima A, Namba T. 1998. A numerical simulation of the circulation in the South China Sea–Preliminary results. Acta Oceanogr Taiwanica, 37(2): 165–186

Wang Bin, Wu Renguang, Lukas R. 2000. Annual adjustment of the thermocline in the tropical Pacific Ocean. Journal of Climate, 13: 596–616

Yang Haijun, Liu Qinyu. 1998. The seasonal features of temperature distributions in the upper layer of the South China Sea. Oceanologia et Limnologia Sinica (in Chinese), 29(5): 501–507

Zhang Mengning, Liu Jinfang, Mao Kexiu, et al. 2006. The general distribution characteristics of thermocline of China Sea. Marine Forecasts (in Chinese), 23(4): 51–58

Zhou Faxiu, Ding Jie, Yu Shenyu. 1995. The intraseasonal oscillation of sea surface temperature in the South China Sea. Journal of Ocean University of Qingdao (in Chinese), 25(1): 1–6

Zhou Yanxia, Fan Zhenhua, Yan Wenbin, et al. 2004. Thermocline comparison of SCS using BT and Nansen data. Marine Science Bulletin (in Chinese), 23(1): 22–26